

## Backward-Wave Oscillation Criterion in a Step-Tapered Helix Travelling-Wave Tube

S.K. Datta, S. Sinha, P. Raja Ramana Rao, S.U.M. Reddy, and Lalit Kumar

*Microwave Tube Research & Development Centre, Bangalore-560 013*

### ABSTRACT

Analysis of backward-wave oscillation criterion is one of the essential steps for designing a broadband travelling-wave tube (TWT) amplifier. In this paper, a methodology for the analysis of the backward-wave oscillation criterion in a helix travelling-wave tube has been proposed with emphasis on its usage as a design tool. The analysis is also extended for a slow-wave structure having distributed RF loss and a closed-form equation has been proposed for calculating the critical interaction length. The analysis is further extended for a step-tapered TWT with distributed circuit loss included in the analysis. The method is finally applied to design a typical slow-wave structure used in an X-Ku band TWT having a step-tapered output circuit.

**Keywords:** Backward-wave oscillation, helix travelling-wave tube, slow-wave structure, step-taper circuit, TWT, amplifier design, travelling-wave tube.

### NOMENCLATURE

$a$	Helix tunnel radius
$\alpha_0$	Maximum growth-rate of the device
$\alpha_n$	Growth-rate of the $n^{\text{th}}$ taper section
$b$	Radius of the electron beam
$\beta_0$	Propagation constant of a uniform circuit
$\beta_{0n}$	Propagation constant of the $n^{\text{th}}$ taper section
$\beta_e$	Beam propagation constant
$\beta_p$	Plasma propagation constant
$\beta_q$	Reduced plasma propagation constant
$C$	Pierce's gain parameter
$CN$	Normalised circuit length
$(CN)_{critical}$	Normalised critical length of the circuit for oscillation to start
$D$	Normalised taper strength
$\epsilon_0$	Permittivity of free-space
$\eta_e$	Charge-to-mass ratio of an electron at rest
$G$	Backward-wave gain of the device
$I_b$	Beam current
$I_{critical}$	Critical current for oscillation to start
$\tilde{I}_n$	Modified Bessel function of first-kind of order $n$
$I_{ST}$	Critical current for a tapered circuit for oscillation to start
$I_{SNT}$	Critical current for a non-tapered uniform circuit for oscillation to start
$K_0$	Interaction impedance for forward space-harmonic mode

$K_{-1}$	Interaction impedance for backward space-harmonic mode
$\tilde{K}_n$	Bessel function of second-kind of order $n$
$L$	Total interaction length
$L_{critical}$	Critical length of the circuit for oscillation to start
$L_{dB}$	Total loss of the circuit in decibel
$L_n$	Length of the $n^{\text{th}}$ taper circuit
$\lambda_e$	Electronic wavelength
$\lambda_g$	Guided wavelength in the circuit
$m$	Taper ratio $L_1/L$
$p$	Helix pitch
$QC$	Pierce's normalised space-charge parameter
$R$	Plasma frequency reduction factor
$\rho_0$	Charge density of the un-modulated electron beam
$u_0$	Electronic velocity of the un-modulated electron beam
$V_b$	Beam voltage
$\omega$	Operating frequency in radians
$\omega_p$	Plasma frequency in radians
$\omega_q$	Reduced plasma frequency in radians

### 1. INTRODUCTION

Helix traveling-wave tubes are unmatched due to their broadband capabilities. However, one of the limiting factors of broadband operation is the occurrence of backward-wave oscillation (BWO) near the upper band-edge, where the slow space-charge wave experiences a  $\pi$ -phase per period leading to positive backward-feedback<sup>1-4</sup>. Thus, BWO suppression is essential for achieving multi-octave bandwidth

in a helix TWT. Backward-wave oscillation instability is conventionally managed in three ways: (i) suitably tailoring the circuit phase velocity to couple the backward-wave with the fast space-charge wave, (ii) providing frequency selective high attenuation at the oscillation frequency (e.g. meander-line), and (iii) providing a phase-velocity taper in the circuit for lowering the gain of backward<sup>2</sup> wave. Providing a phase velocity taper is the most popularly used method, not only for suppressing the BWO, it primarily helps in enhancing the efficiency at upper band-edge frequencies and reducing second harmonic power output at the lower band-edge frequencies as well. Most popular technique of phase velocity taper has been a step-taper (Fig. 1), with two different helix pitches that split the slow-wave structure (SWS) into two different phase velocity regions. The present study brings out as to how phase-velocity taper in a helical SWS helps in combating the BWO.

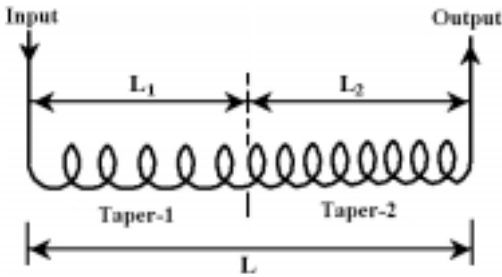


**Figure 1. Schematic of a step-tapered slow wave structure showing two step-tapers having lengths  $L_1$  and  $L_2$  with total circuit length of  $L$ .**

## 2. ANALYSIS

The BWO is a spontaneous phenomena and the onset of the BWO takes place inside the interaction region (away from the input to a distance known as critical interaction length) towards the input (opposite to the direction of electronic flow) that follows a co-sinusoidal pattern having peak at the input with the zero location at the starting point<sup>3,5,7</sup>. The co-sinusoidal pattern defines the oscillation criterion under no-loss, corresponding to the maximum gain (at the maximum growth rate  $\alpha_0$ ) for an interaction length  $L_{critical}$  (the starting point of oscillation), as

$$\cos(\alpha_0 L_{critical}) = 0 \quad \text{whence} \quad \alpha_0 L_{critical} = \frac{\pi}{2} \quad (1)$$

$$\text{where} \quad \alpha_0 = \frac{\beta_e C}{2(QC)^{\frac{1}{4}}}$$

The Eqn. (1) is further simplified to give the critical length for oscillation to start as

$$L_{critical} = \frac{\pi(QC)^{\frac{1}{4}}}{\beta_e C} \quad \text{or, alternatively}$$

$$(CN)_{critical} = \frac{1}{2} \sqrt[4]{QC} \quad (2)$$

$$\text{where} \quad QC = \frac{R^2 \omega_p^2}{4\omega^2 C^2}, \quad C = \left( \frac{K_{-1} I_b}{4V_b} \right)^{\frac{1}{2}}$$

$$\omega_p^2 = \frac{\eta_e \rho_0}{\epsilon_0} = \frac{\eta_e I_b}{\pi b^2 \epsilon_0 u_0}$$

Here,  $u_0$  is the unperturbed (DC) electronic velocity. The reduction of the plasma frequency occurs due to the presence of conducting boundary at the vicinity of the electron beam, the reduction factor given as<sup>7</sup>

$$R = \left[ 1 - (\beta_e b) \left( \frac{\tilde{I}_1(\beta_e b) \tilde{K}_0(\beta_e a) + \tilde{I}_0(\beta_e a) \tilde{K}_1(\beta_e b)}{\tilde{I}_0(\beta_e a)} \right) \right]^{\frac{1}{2}} \quad (3)$$

Here,  $\tilde{I}_n$  and  $\tilde{K}_n$  are the modified Bessel functions of first- and second- kinds, respectively, of order  $n$ ,  $b$  is the beam radius and  $a$  is the tunnel radius through which the electron beam traverses. However, the effect of distributed loss is not included in the computation of the critical length. This has been introduced by the present authors by a curve fitting to Johnson's results<sup>3</sup> following Grow and Gunderson<sup>8</sup> as

$$L_{critical} = 0.0178 \left( \frac{\lambda_e}{C} \right)^{\frac{1}{4}} \sqrt[4]{QC} \left( 1 + \frac{1013}{L_{dB}^2} \right) \left( \frac{L_{dB}^2}{33} \right) \quad (4)$$

The Eqns. (2) and (4) can be used to compute the critical length of the interaction structure for a uniform loss-less and lossy structure, respectively. Now, a method for computing the critical length for a step-tapered SWS with two sections having different phase velocities has been proposed. For analysing the backward-wave gain of such a tapered SWS, recourse of the two-wave approach of Nilsson<sup>5,6</sup> *et al.* has been taken. The analysis approach is a linear one based on Eulerian hydrodynamical modelling of the electron beam and suits well for BWO analysis, as the BWO interaction is primarily a linear phenomenon where electron overtaking is a rare occurrence<sup>6-7,9</sup>. For the sake of simplicity, loss-less case has been considered, and the backward-wave gain for the tapered circuit is obtained as

$$G = \frac{\exp(j\beta_0 L)}{\left( \prod_{n=1}^2 A_n + \prod_{n=1}^2 C_n \right)} \quad (5)$$

where

$$A_n = \cos(\alpha_n L_n) - j \left\{ \left( 1 - \alpha_0^2 / \alpha_n^2 \right)^{\frac{1}{2}} \sin(\alpha_n L_n) \right\} \cdot \text{sgn}(\beta_{0n} - \beta_e - \beta_q)$$

$$C_n = -j(a_0/a_n) \sin(a_n L_n)$$

$$\alpha_n = \alpha_0 \left\{ 1 + (-1)^n D(2\alpha_0 L)^{-1} \right\}^{\frac{1}{2}}$$

Here,  $\beta_q (=R\omega_p/u_0)$  is the reduced plasma propagation constant,  $\alpha_{0is}$  the Pierce's maximum growth parameter, and  $D=|\Delta\beta_0|L$  is the normalised taper strength.

For probable backward-wave instability, the gain must shoot up making the denominator of Eqn. (5) as zero, in which case the BWO start condition is obtained from the first zero of the real part of the denominator ( $A_1A_2 + C_1C_2$ ) as

$$\prod_{n=1}^2 \cos(\alpha_n L_n) + \prod_{n=1}^2 (1 - \alpha_0^2 / \alpha_n^2)^{\frac{1}{2}} \sin(\alpha_n L_n) - \alpha_0^2 \prod_{n=1}^2 \sin(\alpha_n L_n) / \alpha_n = 0 \quad (6)$$

This equation is solved in a digital computer for the first root of  $\alpha_0 L$  for a given value of normalised taper strength  $D=|\Delta\beta_0|L$ . The lengths of the tapered sections  $L_n$  are considered as  $L_1 = mL$  and  $L_2 = (1-m)L$  with  $m$  defined as the ratio of taper lengths.

The first root of this equation  $\alpha_0 L$  as obtained is then interpreted for a parameter ( $2\alpha_0 L/\pi$ ), which depends on BWO start oscillation current as<sup>5</sup>.

$$\frac{2\alpha_0 L}{\pi} = \sqrt[4]{\frac{I_{ST}}{I_{SNT}}} \quad (7)$$

Here,  $I_{ST}$  is the start oscillation current for a tapered circuit, and  $I_{SNT}$  is the start oscillation current for a non-tapered single pitch circuit, both the circuits are considered to be loss-less and having the same total lengths. It is worth noting here that the oscillation-induced instability is a spontaneous process that occurs at a frequency where the circuit phase velocity and the slow space-charge wave have  $\pi$ -phase per period at perfect synchronism satisfying  $\beta_{0n} - \beta_e - \beta_q = 0$  and  $\beta_{0n} p = (\beta_e + \beta_q) p = \pi$ . However, for the brevity, it was considered that the oscillation takes place at a frequency that corresponds to the mean frequency of the two taper sections, i.e.,  $\beta_0 p = (\beta_e + \beta_q) p = \pi$  such that  $\beta_0 = (\beta_{01} + \beta_{02})/2$ .

For all such computations, one needs to know the phase-velocity and interaction impedance of the backward-wave space-harmonic mode at the  $\pi$ -point frequency. One can easily compute the phase velocity and the interaction impedance of the fundamental space-harmonic mode using eigen-mode solutions through 3-D electromagnetic analysis in HFSS, MAFIA or CST Microwave Studio. However, computation of interaction impedance at the backward-wave space-harmonic mode needs an analytical formulation (see *Appendix*)<sup>1</sup>, given as

$$K_{-1,r} = K_{0,0} \times \left( \frac{k_0 a}{1 - k_0 a} \right) \left( \frac{\tilde{I}_0^2 \{ \beta_0 a \}}{\tilde{I}_1^2 \{ \beta_{-1} a \}} \right) \times \tilde{I}_1^2 \{ \beta_{-1} r \} \quad (8)$$

Here,  $\tilde{I}_n$  and  $\tilde{K}_n$  are the modified Bessel functions of first- and second- kind, respectively, of order  $n$ .

### 3. RESULTS AND DISCUSSION

For numerical appreciation of the problem, the SWS used in a typical X-Ku band helix TWT was considered. The SWS is a metal-segment loaded one in which the helix

is supported inside a metallic barrel using three rectangular APBN support rods. The tube operates at a beam voltage of 10 kV with a micro-perveance of 0.4 having an average beam radius of 0.40 mm. The SWS is made in three sections: the input section has a uniform pitch of  $1.53a \pm 0.005$  mm; the middle section also has a uniform pitch of  $1.59a \pm 0.005$  mm; whereas the output section has a step-taper having two pitches,  $1.59a \pm 0.005$  mm and  $1.53a \pm 0.005$  mm with a 4 turn transition (normalised with respect to the helix tunnel radius  $a$ ). The phase-velocity and interaction impedance of the forward propagating mode have been computed using 3 D HFSS modeling. These values have been interpreted for the backward-space harmonic mode using the formulation presented in this paper and subsequently used to analyse the backward-wave effects. The  $p = 1.53a$  pitch section has the  $\pi$ -point frequency of 19.98 GHz at which the normalised phase velocity is 0.175 with forward space-harmonic interaction impedance of 3.55 ohm, and the  $p = 1.59a$  pitch section has the  $\pi$ -point frequency of 20.06 GHz at which the normalised phase velocity is 0.180 with forward space-harmonic interaction impedance of 3.34 ohm.

The backward space-harmonic interaction impedance for the structure has been computed using Eqn (8), which is plotted in Fig. 2 as a function of beam-filling factor. It can be seen that as the beam-filling increases, the backward-wave interaction impedance increases sharply, thereby increasing the possibility of higher backward-wave gain, and hence, a lesser critical length.

The backward-wave interaction impedance thus computed has been used to compute the critical lengths of the different pitch sections using Eqn (4) for a circuit loss of 2 dB/in at the  $\pi$ -point frequencies, as shown in Fig. 3 and Fig. 4. It can be seen that as the beam current increases, the critical length for oscillation to start reduces, and vice versa. The critical length reduces as the beam-filling factor increases; this is because increase in beam-filling increases the electric field threading the beam, thereby increasing the backward-wave interaction, as seen in Fig. 2. However, as one can expect an increase in the current density due to bunching of electrons in the beam and consequence to that, an increase in the beam filling, the design of the critical length must consider an increased beam-filling.

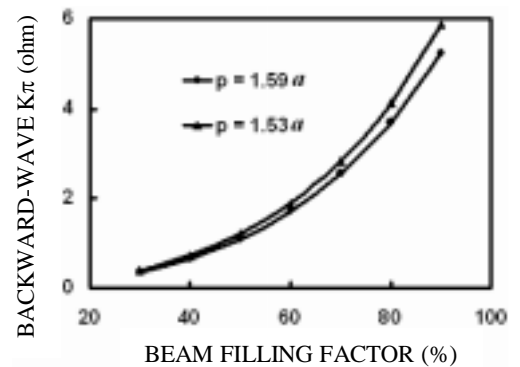


Figure 2. Backward-wave interaction impedance of the structure versus beam-filling factor as computed using Eqn (8).

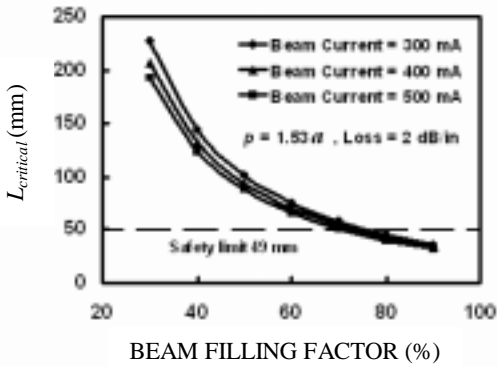


Figure 3. Critical length versus beam-filling factor for input section with operating beam current as the parameter.

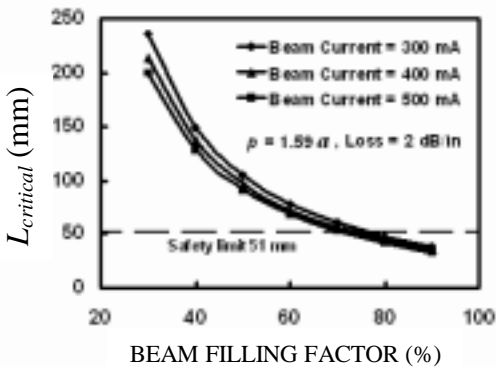


Figure 4. Critical length versus beam-filling factor for middle section with operating beam current as the parameter.

Thus, the safe critical lengths have been arrived at for the 65 per cent beam filling and the input-section ( $p = 1.53a$ ) and middle-section ( $p = 1.59a$ ) lengths have been designed accordingly as  $L_{input} = 16.81\lambda_g \pm 0.1$  mm and  $L_{middle} = 12.26\lambda_g \pm 0.1$  mm, respectively. Figure 5 shows an alternative representation of the results for the middle section, where one would be very easily able to appreciate the effects of beam filling both in terms of critical current and critical length. It can be seen that the critical length and the critical current show a logarithmic dependence.

Next, the effect of circuit loss on the critical length (Fig. 6) was analysed. It is observed that the circuit loss

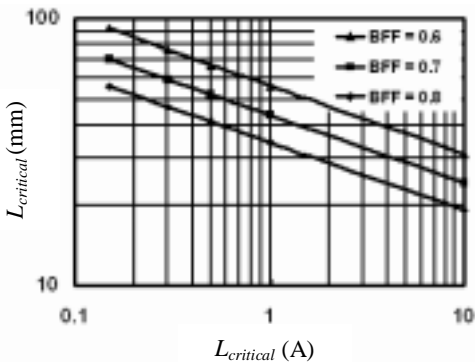


Figure 5. Critical length versus critical current showing a logarithmic dependence with beam-filling factor as parameter.

indeed increases the critical length; however, the improvement is not significant. It is seen that an increase of loss by 9 dB/in could increase the critical length only by around 10 per cent. This led to the conclusion that distributed loss may not be an efficient way towards combating BWO; however an efficient way may be the use of a lumped loss in the circuit to provide a break in the growth of the backward-

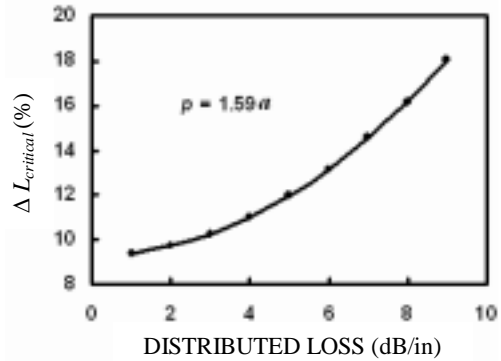


Figure 6. Increase in critical length versus distributed circuit loss.

wave interaction.

Next, the effect of pitch taper at the output section was investigated. The normalised start oscillation currents for different taper positions of the circuit are shown in Fig. 6. It was assumed that the relative phase velocity difference between the two tapers is the same for both the forward-wave and the backward-wave modes. This is a valid assumption as the taper is obtained simply by providing a change in helix pitch in the axial direction. It may be observed from Fig. 7 that the taper length at the proportion of 50 per cent – 50 per cent gives the best oscillation suppression, whereas a taper at the proportion of 70 per cent – 30 per cent reduces the threshold oscillation current below the threshold current of that of an un-tapered circuit. For the circuit under consideration, the output section (being  $L = 23.69\lambda_g$  long) has two-step pitch-tapered sub-sections. The sub-sections having two pitches,  $p = 1.59a$  and  $p = 1.53a$  with a 4 turn transition. The taper sections have ~3.2 per cent phase velocity step corresponding to normalised taper

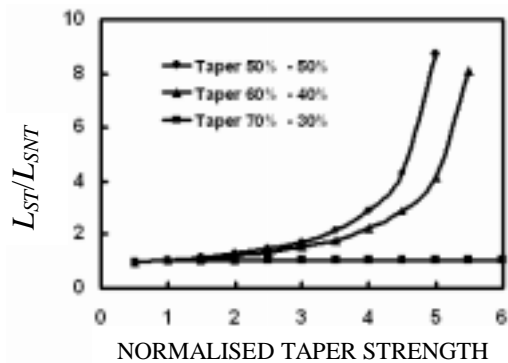
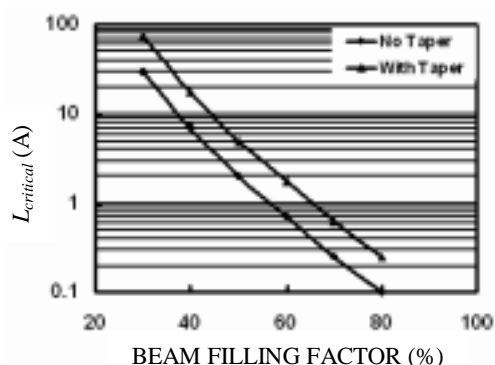


Figure 7. Normalised start oscillation current versus normalised taper strength with the taper proportions as the parameter.

strength  $\sim 4.2 (D)$ . The taper circuit lengths  $L_1=13.60 \lambda_g$  with  $p=1.59a$  and  $L_2=10.09 \lambda_g$  with  $p=1.53a$  corresponds a taper positioning ratio of 58 per cent – 42 per cent.

For the present case of  $D = 4.2$  and a taper ratio of 58 per cent – 42 per cent, the ratio of  $I_{ST}/I_{SNT}$  (start-current taper to start current no-taper) becomes  $\sim 2.5$ , indicating that the start oscillation current increases due to taper by a factor of 2.5 wrt a non-tapered circuit. The increase in the critical beam current versus beam-filling factor is shown in Fig. 8. This shows that the instability in interaction can occur if the entire output interaction circuit operates with around 75 per cent beam filling.



**Figure 8.** Critical current versus beam-filling factor showing the effect of 58% – 42% taper positioning with a normalized taper dispersion step of 4.2.

#### 4. CONCLUSION

A two-wave approach has been proposed to demonstrate the positioning of the phase velocity taper for suppression of BWO in a helix TWT amplifier. The approach is based on loss-less assumption and valid only for backward-wave interaction in a linear regime. However, the procedure is general and one may consider analysing the multi-taper effects and also the effects of distributed loss on the BWO suppression mechanism.

#### REFERENCES

1. Gilmour, A.S. Jr., *Principles of traveling wave tubes*, Norwood: Artech House, 1994.
2. Basu, B.N. *Electromagnetic theory and applications in beam-wave electronics*, Singapore: World Scientific, 1996.
3. Johnson, H.R. Backward-wave oscillators, *In Proc. IRE*, 1955, **43**, pp. 684-97.
4. Heffner, H. Analysis of the backward-wave traveling-wave tube, *In Proc. IRE*, 1954, **42**, pp. 930-37.
5. Nilsson, O. & Hangstrom, C. A two-wave theory of traveling-wave tubes and backward-wave oscillations, *IEEE Trans. Electron Devices*, 1975, **22**, 869-80.
6. Tsutaki, K.; Yuasa, Y. & Morizumi, Y. Numerical analysis and design for high performance helix traveling-wave

tubes, *IEEE Trans. Electron Devices*, 1985, **32**, pp.1842-49.

7. Rowe, J.E. *Non linear Electron-wave interaction phenomena*, Academic Press, New York and London, 1965.
8. Grow, R.W. & Gunderson, D.R. Starting conditions for backward-wave oscillators with large loss and large space charge, *IEEE Trans. Electron devices*, 1970, **17**, 1032-39.
9. Antonsen, T.M. Jr.; Safier, P.; Chernin, D.P. & Levush, B. Stability of traveling-wave amplifiers with reflections, *IEEE Trans. Plasma Science*, 2002, **30**, 1089-107.
10. Datta, S.K.; Kumar, L.; Kumar, S. & Basu, B.N. Large-signal analysis for BWO start condition in helix TWTs, *In Proc. Intl. Vacuum Electronics Conference*, Seoul, 2003.

#### Contributors



**Dr S.K. Datta** received his BE in Electronics and Tele-communications Engineering in 1989 from the Bengal Engineering College, Calcutta University, India, and the MTech and PhD in Microwave Engineering in 1991 and 2000, respectively, from the Institute of Technology, Banaras Hindu University, Varanasi, India. His current areas of research include the computer-aided design and development

of helix and coupled cavity traveling-wave tubes, Lagrangian analysis of the nonlinear effects in traveling wave tubes and the studies on electromagnetic wave propagation in chiral and bi-isotropic media. He is a Fellow of the IETE of India and a member of Magnetics Society of India. He is the founder General Secretary of Vacuum Electronic Devices & Applications Society (VEDAS), India. He is currently working as a Scientist in the Microwave Tube Research and Development Centre, Bangalore, India. He received Sir C. Ambashankaran Award of Indian Vacuum Society for Best Paper (1998), INAE Young Engineer Award (2000), Sir C.V. Raman Young Scientist Award (2002) and DRDO Agni Award for Excellence in Self Reliance (2003).



**Mr P. Raja Ramana Rao** received his BE in Electronics and Communication Engineering in 1997 from the V. R. Siddhartha Engineering College, Nagarjuna University, India. He is currently working as Scientist at MTRDC, Bangalore. His research area includes computer-aided design and development of helix traveling-wave tubes. He is a member of the Vacuum Electronic Devices & Applications

Society (VEDAS), India and a member of the Magnetics Society of India. He received DRDO Young Scientist of the Year Award (2005).



**Mr S. Umamaheshwara Reddy** received his BE in Electronics and Telecommunications Engineering in 1983 and the MTech in Microwave Engineering in 1986 from the Osmania University, India. He is currently working as Scientist at MTRDC, Bangalore. His research area includes computer-aided design and development of helix and coupled cavity traveling-wave tubes. He is a Fellow of the Vacuum Electronic Devices & Applications Society (VEDAS), India and a member of the Magnetics Society of India. He received DRDO Scientist of the Year Award (2001) and DRDO Agni Award for Excellence in Self-Reliance (2003).



**Dr Lalit Kumar** received his MSc in Physics from Meerut University and PhD (Physics) from Birla Institute of Technology & Science, Pilani, India. He is the Director of MTRDC, Bangalore. His current interests include: TWTs, microwave power modules & ultra-broadband high-power microwave devices. He is a Fellow of IETE & a Member of Indian Physics Association, Indian Vacuum Society, Indo-French Technical Association, and Magnetics Society of India. He is the founder President of Vacuum Electronic Devices & Applications Society (VEDAS), India. He received JC Bose Memorial Award of IETE for Best Paper in 1993, Best Project Award of CEERI in 1993 & IETE-IRSI (83)-2001 Award, DRDO Agni Award for Excellence in Self-Reliance (2003).

## Appendix

### Backward-Wave Interaction Impedance

We need to calculate the backward-wave ( $-1$  space harmonic) interaction impedance at a particular radial location inside the beam, from a known value of on-axis fundamental interaction impedance, for which a closed form approximate analytical equation is presented here. This derivation stems from the basic formulation of Watkins and Ash used by Johnson<sup>3</sup> that the ratio of both the impedances at the helix is given as:

$$R_k = \frac{K_{-1,a}}{K_{0,a}} = \frac{k_0 a}{1 - k_0 a} \quad (\text{A.1})$$

Here,  $k_0$  is the free space propagation constant at the frequency of interest. We now define the axial electric field distribution along the radial direction as follows:

$$E_{r,0} = A I_0 \{ \beta_0 r \} \quad \text{and} \quad E_{r,-1} = B I_1 \{ \beta_0 r \} \quad (\text{A.2})$$

whence from (A.1) we get,

$$B^2 = R_k A^2 \frac{I_0^2 \{ \beta_0 a \} \beta_{-1}^2}{I_1^2 \{ \beta_{-1} a \} \beta_0^2}$$

Eliminating field constants from (A.2), we get the backward-wave ( $-1$  space harmonic) interaction impedance at any radial location inside the helix as:

$$K_{-1,r} = K_{0,0} \times \left( \frac{k_0 a}{1 - k_0 a} \right) \left( \frac{I_0^2 \{ \beta_0 a \}}{I_1^2 \{ \beta_{-1} a \}} \right) \times I_1^2 \{ \beta_{-1} r \} \quad (\text{A.3})$$

Here, all parameters are to be calculated at the  $\pi$ -point frequency. Expression (A.3) for the interaction impedance is appropriate for a thin beam around the axis of the structure. In the case of a thick solid beam of radius  $r$ , it would be more appropriate to use the average electric field intensity over the electron beam cross-section. This would introduce an additional factor  $\left( 1 - \left( I_n' \{ \beta_n r \} / I_n \{ \beta_n r \} \right)^2 \right)$  in the right-hand-side of (A.3), for the given  $n$ th space-harmonic propagating mode.